Title

ANGLE-RESOLVED PHOTOEMISSION DETERMINATION OF A-LINE VALENCE BANDS IN Pt AND Au USING SYNCHROTRON RADIATION

Author

Mills, K.A.

Publication Date

1979-07-01

Lawrence Berkeley Laboratory
UNIVERSITY OF CALIFORNIA

Materials & Molecular Research Division

Submitted to Physical Review B

ANGLE-RESOLVED PHOTOEMISSION DETERMINATION OF Λ-LINE VALENCE BANDS IN Pt AND Au USING SYNCHROTRON RADIATION

K. A. Mills, R. F. Davis, S. D. Kevan, G. Thornton, and D. A. Shirley

July 1979

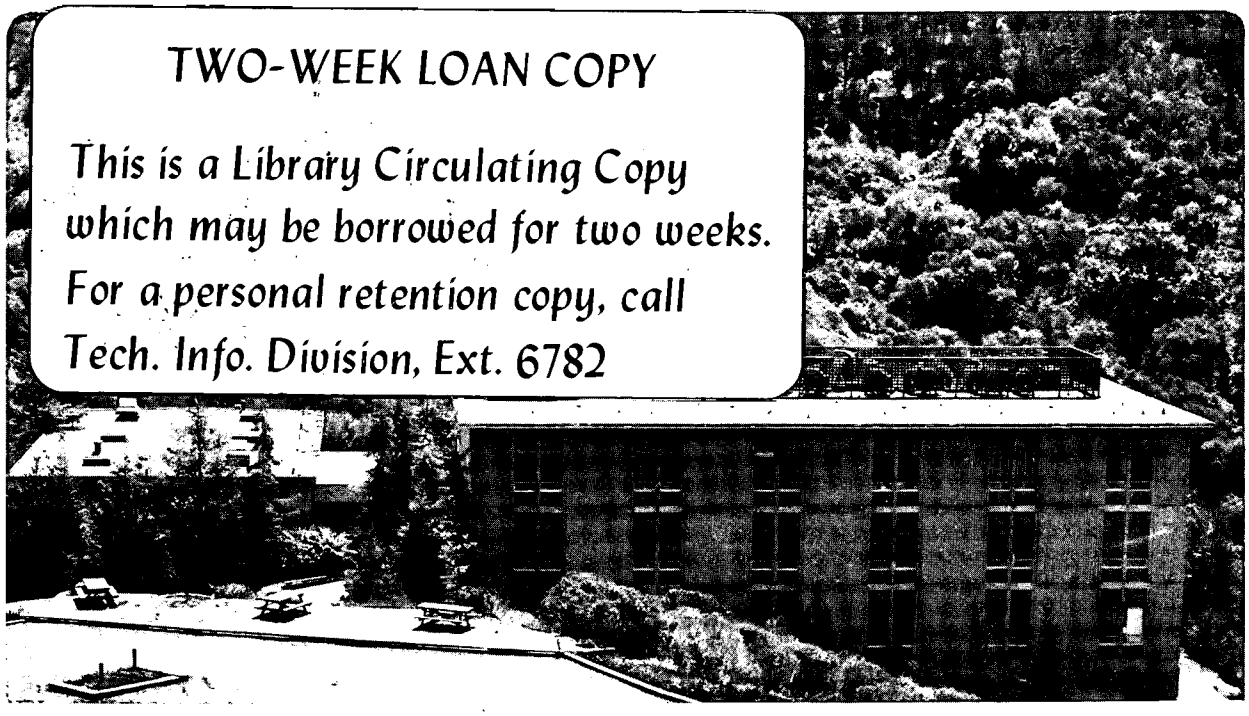

Prepared for the U. S. Department of Energy
under Contract W-7405-ENG-48

DISCLAIMER

ANGLE-RESOLVED PHOTOEMISSION DETERMINATION OF Λ-LINE VALENCE BANDS IN Pt AND Au USING SYNCHROTRON RADIATION

K.A. Mills, R.F. Davis, S.D. Kevan, G. Thornton and D.A. Shirley

Materials and Molecular Research Division
Lawrence Berkeley Laboratory
and
Department of Chemistry
University of California
Berkeley, California 94720

July 1979

ABSTRACT

Angle-resolved photoemission spectra are reported for Au(111) and Pt(111) in the photon energy range $6 \leq h\nu \leq 33$ eV. Experimental dispersion relations along Λ were derived for both crystals; comparison with RAPW calculations showed generally good qualitative agreement, but quantitative disagreement of the order of a few tenths of an eV. Band energies are tabulated; values at Γ are Γ_8 = 3.55, 5.90, Γ_7 = 4.45 eV for Au; Γ_8 = 1.40, 4.07, Γ_7 = 2.80 eV for Pt. The s-band is found to be ca. 1 eV (Pt) and 0.5 eV (Au) less bound than the theoretical prediction. Ligand field parameters at Γ are presented for both samples: $\xi(5d) = 0.71 \pm .05$ eV, $10Dq = 1.22 \pm .05$ eV for Au; $\xi(5d) = 0.66 \pm .05$ eV, $10Dq = 1.78 \pm .05$ eV for Pt. The systematics of 10Dq in the noble metals is discussed. The polarization dependence of the spectra was used to assign initial state symmetries empirically:

$6 \leqslant h\nu \leqslant 33$ eV. This range of energies enables the determination of the valence-band structure along most of the Λ line, and in particular allows the determination of the d-band energies at Γ. In addition, we have investigated the influence of radiation polarization for Pt(111), and of temperature for Au(111). Final-state effects have also been studied, with particular attention to the choice of the final state, the nature of intensity resonances, and the appearance of a constant-kinetic-energy feature. As will be discussed in detail, all of these effects have their counterparts in the 3d and 4d metals cited above, and all can be understood within the current theoretical framework of ARP.

Section II describes our experimental procedures. In Section III we discuss the dispersion relations obtained, and estimate crystal field parameters. Polarization effects are considered in Section IV, and the influence of temperature is elucidated in Section V. Section VI is devoted to final-state effects, and the last section provides a summary of our results.

II. Experimental

High-purity crystals of Au and Pt were cut to produce (111) surfaces, and were subsequently polished to 1-micron roughness and etched. The Pt crystal was then installed in a ultrahigh vacuum chamber and cleaned of bulk impurities by a combination of repeated Ar^+ sputtering/annealing cycles

and heating in 10^{-6} torr of O_2. Cleanliness was monitored by Auger spectroscopy (AES). Both crystals were then mounted for experimentation (orientation to 1° or better as determined by back-reflection Laue photography). Final cleaning just prior to data acquisition was performed in situ by Ar^+ bombardment and annealing at 600°C (Au) and 700°C (Pt); the Pt sample was characterized by both LEED and AES, and the Au sample by AES.

The photoemission measurements were performed on the 8° branch of Beam Line I at the Stanford Synchrotron Radiation Laboratory. The apparatus used for Au has been described elsewhere,[7] the only modification being a reduction of the angular acceptance of the CMA to $\pm$ 2.5°. The electric field vector of the incident radiation lay in the horizontal plane defined by the Poynting vector of the light and the electron propagation direction; the angle between the latter two was fixed at 63°. In studying Pt(111), a chamber was employed which incorporates a 5.40 mean radius hemispherical analyzer with an angular acceptance of $\pm$3°, mounted to allow rotation through 2π steradians.[8] For "s-polarized" spectra, the sample was rotated so that the $\vec{E}$ vector of the light was parallel to the (111) face, the photon propagation direction ($\vec{k}_\gamma$) being at 60° relative to the normal. For "p-polarized" light, the $\vec{E}$ vector was effectively rotated 90° from this orientation by moving the sample and analyzer, the angle between $\vec{k}_\gamma$ and normal again being 60°. The analyzer was then positioned

for detection of electrons propagating normal to the crystal surface. The geometry of each experiment is shown in Figure 1.

Base pressures in both chambers were typically in the 10^{-10} torr range. Samples were oriented in situ using laser collimation, and the normal was determined to 1° or better. The energy resolution (monochromator plus analyzer) varied from ca. 0.1 eV at low-photon energies to ca. 0.2 eV at the high-energy limit. Count rates were excellent, typically on the order of 10^3 to 10^4 sec^{-1}, and a spectrum with adequate statistics could be obtained in 5 to 10 minutes.

Spectra for the entire energy range are shown for Au and Pt (p-polarized radiation) in Figures 2 and 3.

III. Dispersion Relations

Before proceeding with the actual determination of the $E_n(\vec{k})$ relationships, we will discuss the spectra with a view toward identifying the major mechanisms involved.

In accord with previous results,[5] a surface state peak for Au(111) appears at 0.2 eV binding energy; it rapidly diminishes in intensity with increasing photon energy and by $h\nu$ = 16 eV has essentially disappeared. A (111) face surface state has also been observed in Cu and Ag, and general criteria for its existence have been discussed by Heimann et al.[9] Our binding energy is 0.2 eV less than that reported by Hansson and Flodstrom; this discrepancy will be discussed below.

While density-of-states features do not play a dominant role in the spectra, they may be identified in two cases. For both Pt and Au, a dispersionless shoulder is seen on the leading edge of the d-bands ($E_B \sim 0.3$ eV for Pt, 2.7 eV in Au). No RAPW density of states (TDOS) is available for Pt; for gold, when one includes the difference in energy zero between our measured bands and the theoretical ones, this feature agrees well with the prediction of a TDOS feature at $E_B = 2.4$ eV.[10] This is the only TDOS feature expected; the others would either coalesce under the much stronger direct transitions of similar energy, or be unobservable due to a low cross-section (high s-like initial-state character). This peak grows in relative intensity with increasing photon energy, which results from a decrease of the electronic mean-free path, leading to a breakdown in k-conservation and an enhanced surface DOS contribution. This surface contribution has been studied by Citrin et al. in gold,[11] where it was found to be shifted to 0.4 eV lower binding energy relative to the bulk; the growth of this TDOS feature in our spectra would then be consistent with an enhanced surface contribution, the bulk contribution coalescing with the much stronger direct-transition peak. For platinum, the feature at 0.3 eV behaves analogously. A possible origin of this feature is band 6 along the Q line, which is very flat between W and L. Further evidence for the TDOS vs one-dimensional density of states (ODDOS) nature of this peak may be inferred

from its behavior on cooling, as discussed below. Such a shoulder has also been seen in Cu and Ag.[1,4]

Whenever a flat initial-state band exists, as is the case here for band 2, the possibility of ODDOS features must be considered. While at photon energies of $h\nu \leq 18$ a ODDOS peak due to $\Gamma(2,3)$ will not affect our assignment, since it will be clearly separated from the direct transition feature, for higher energies these features can coalesce. As discussed below in the section on temperature dependence, it seems that some of the contribution to the 6.2 eV peak in gold at 18 eV is due to a ODDOS mechanism. This could conceivably cause some error in the experimentally derived location of band 2 near the regions where it begins to disperse, but the error is small and easily correctable if this possibility is kept in mind. In the spectra of the (111) face, in fact, little ODDOS behavior is apparent; for the other low-Miller-index faces, however, the situation is considerably more complicated.[5]

The behavior of the "s-p" plateau was discussed previously,[1,4] and we comment on it only briefly here. For both Ag and Cu, this feature varied in intensity, reaching a minimum for photon energies corresponding to final states near Γ. Such behavior was observed in this study as well, with the s-p band to d band intensity ratio decreasing by roughly one order of magnitude from $h\nu = 9$ eV (3/4 of the way along Λ to Γ) to $h\nu = 21$ eV (near Γ). We shall return

to this feature in Section V.

A constant kinetic energy feature is also apparent for both crystals, in analogy with results for Ag(111)[4] and Pd(111).[3] For Au, its onset in the spectra is most clearly visible starting for $h\nu$ = 26 eV, while in Pt it appears first as a shoulder on the 4.0 eV peak at $h\nu$ = 23 eV. Wider energy scans were taken of Pt at photon energies up to 30 eV to confirm the continued presence of the feature, but they are not presented here.

By far the largest portion of the sharp spectral features observed can be assigned to direct transitions. Our spectra agree well with those of Heimann et al. at $h\nu$ = 16.85 eV, and Hansson and Flodstrom[5] for the range $7.0 \leq h\nu \leq 11.6$ eV, with the exception of the location of E_f in the latter. We have assigned these transitions as follows:

1. Relative binding energies were established by spline-fitting the experimental data and visually fitting overlapping peaks as necessary.

2. Band 7 in the theoretical RAPW calculation for gold, which has largely $\vec{G}$ = [888] character (we use the notation of Ref. 10, in which Γ = (000), and L = (444)) in the middle of the zone, was fitted in this region to the free-electron-like equation $E(k) = h^2k^2/2m^* + V_o$, with the reduced mass m^* and valence-band minimum V_o as free parameters. This yielded $m^* = 1.17\ m_e$ and $V_o = -3.2$ eV. The fitted final state was then used in the standard way[4] to obtain initial

state momenta; for this photon energy range, $\vec{G}$ = [888] connects all initial and final states. It was found that such an approach gave somewhat better results than the choice of a true free-electron parabola with V_o given by $\Gamma(1)$, although the difference was close to the limits of k-resolution in the experiment. For platinum, no theoretical RAPW final-state bands have been reported[12]; accordingly, the fitted Au final state was used, scaled by the ratio of the lattice constants, with the zero of energy shifted to account for the difference in E_F. We feel this procedure is justified given the close similarity of the initial-state theoretical dispersion relations for both materials when this procedure is followed.

3. The Fermi level in Au was taken as the energy at half-height on the onset of the s-p plateau for those photon energies where such an assignment was unambiguous. For $h\nu \leq 16$ eV, however, this onset was masked by the surface state at 0.2 eV; for these spectra, careful monitoring of the analyzer reference voltage enabled assignment of E_F via comparison of these voltages. The work functions so derived showed an RMS scatter of $\pm$ 0.05 eV, and our binding energies at $h\nu$ = 17 eV agreed with those of Heimann et al.[6] at 16.85 eV to within 0.07 eV. Accordingly, we feel that the binding energies of Hansson and Flodstrom, which are generally 0.2 eV greater than ours, are too large due to the difficulty in assigning E_F with only low-photon energy data.

In the case of Pt, an analogous approach was employed, except that no surface state was present, while the TDOS feature at 0.3 eV served as its surrogate in masking E_F. At low and high energies, however, this shoulder either vanished or became a well-defined peak; in either case, E_F could then be assigned and analyzer voltages used to set E_f for other energies. With the use of spectra for $h\nu \leq 11$ and $h\nu \leq 28$, the derived work function had an RMS scatter of $\pm$ 0.03 eV. The agreement between the s-polarized and p-polarized data was in general excellent ($\leq$0.1 eV difference).

As shown in Figures 4 and 5, our data give smooth variations of E with $\vec{k}$ for both crystals, and all the bands are observed in at least part of the zone. The band energies are tabulated in Table I for selected values of $\vec{k}$; our data may be recovered from Figures 4 and 5 by using k^2 and E_B to back-calculate $h\nu$, with $E(k) = h\nu - E_B$. The assignment of the band 1 transitions in Pt, which are admittedly weak in these spectra, was aided by additional data from higher ($h\nu \geq 40$ eV) energy spectra[13]; all other transitions, however, were easily assigned with the lower-energy data. For simplicity, we have not included on this plot either the surface-state or indirect-transition peaks described earlier. Band 4 in Pt cannot be assigned for p-polarization radiation near Γ because the spectra are dominated by the band 2,3 and 5,6 features for these photon energies, but an assignment can be made from s-polarized light spectra and will be

presented below. It appears that there is a need to adjust the theoretical energy zero in gold by approximately 0.2 eV down to fit our results. This discrepancy is attributable to the use of the 4.2°K lattice constant in the original RAPW calculation. Subsequent work[14] using the 300°K value has shown a shift "of the majority of the bands" by ca. 0.2 eV down. This is consistent with our observations; further, in the case of Pt, where the RAPW calculation is for a 300°K crystal, no shift is suggested by our data. From the band energies at Γ, given in Table I, it follows that the $(\Gamma_8 - \Gamma_8)$ splitting in both Pt and Au is virtually identical to theory, while Γ_7 is too close to the upper Γ_8 level by about 0.15 eV in both cases. Most likely, these discrepancies in the theory are due to difficulties in calculating the spin-orbit interaction, and in determining E_F.

By far the most dramatic difference between theory and experiment occurs in the actual shape of the bands mapped. For both crystals, bands 5,6 have a larger splitting than predicted, and for $\vec{k}$ nearer to Γ than expected. Also, bands 3,4 do not repel near (5,5,5) as much as the theory would suggest. That this behavior occurs in both crystals gives us confidence in its certitude, and precludes its being due to an artifact of our analysis, such as a poor choice of final state. It is important to note that these features are insensitive to the exact nature of the final state; while a variation in the final state used will alter the region

of the zone in which the effects occur, it cannot alter the relative splittings or absolute energies of the peaks, and the discrepancies will remain. In addition, our quasi-free-electron final state fits the RAPW conduction band quite well midway along Λ, where much of the discrepancy is observed. This behavior is not observed in Ag(111), but in Pd(111)[3] the (5,6) splitting is characteristically 0.2 eV larger than predicted; band 3(Λ_3) is not obtained for this crystal along all of the Λ line, but the results presented strongly suggest that band 4(Λ_1) also extends to significantly lower binding energies midway along Λ than is theoretically predicted. It is interesting to note that the relativistic KKR calculation of Sommers and Amar[15] for Au shows some qualitative similarity with the band 3-band 4 narrowing observed near (5,5,5), and the larger band 5-band 6 splitting observed; however, their d-band width is much too large due to the use of 2/3 Slater exchange, and XPS measurements[16] have shown the work of Christensen and Seraphim to give much better agreement with the photoemission density of states.

From the band energies at Γ, we may also derive crystal field parameters, as discussed in our Ag(111)[4] paper. These results are presented in Table II. For Pt(111), the band energies at Γ were assigned using the data for s-polarized radiation, which enabled the assignment of band 4 up to 24 eV, corresponding to an initial state wavevector of magnitude $|k|^2 \sim 187$ for this binding energy. The comparison of ξ_{5d}

with that obtained in atomic structure calculations[17] is excellent for both Pt and Au, within roughly 4% of the predicted value. This agreement is in part fortuitous, as ξ will be different in the solid state, and in fact may be expected to depend on the binding energy of the associated band as well. As discussed in Anderson's theoretical paper on Pt,[12] ξ is expected to vary from ca. 0.54 eV to 0.76 eV; using the theoretical energies at Γ, however, gives results that are significantly different from those obtained experimentally, and actually produces a value of ξ_{5d} for Pt that is greater than that for Au, in qualitative as well as quantitative disagreement with the atomic values. These considerations suggest that the presently available theoretical calculations are not incorporating the spin-orbit interaction in a satisfactory manner, or that the crystal potential used is sufficiently in error to produce these discrepancies.

It is interesting to compare values of 10Dq for the group VIII and IB transition metals. Using our results in combination with values of critical points reported in the ARP literature, we have compiled 10Dq values for Ni, Cu, Pd, Ag, Pt, and Au (Table III). The empirical Ni value is anomalous, and may be due to an improper assignment of $\Gamma_{25'}$. Overall, however, the trends are obvious and consistent with expectation: 10Dq increases as one proceeds either to the left, or down, in the periodic table.

IV. Polarization Dependence for Pt(111)

In materials such as copper, where relativistic effects are small and the eigenfunctions therefore transform as the single space group of the crystal, it is well-known that an appropriate choice of experimental geometry can allow the observation of initial states of particular symmetry, as determined by the requisite selection rules.[18] Such is also the case for Pt(111), although the situation is more complicated due to spin-orbit coupling, which gives eigenfunctions transforming as the associated double group.

Our results for s- and p-polarized radiation are shown in Figure 6. Let us note first of all that for the "p-polarized" case, the polarization vector $\vec{\eta}$ is in fact a mixture of the two components ($\hat{\eta}_1 \perp [111]$ and $\hat{\eta}_2 \parallel [111]$) with about 60% η_2 character. In addition, the finite angular resolution of the spectrometer will break the selection rules, which can be rigorously derived only for mirror-plane emission. As a consequence, only diminution and not disappearance of peaks can be expected, and this is in fact observed.

The major changes in the spectra are as follows. First, it is seen that the band (5,6) doublet shows much larger intensity variations for s-polarized ($\hat{\eta} \sim \hat{\eta}_1$) radiation, with the 5 to 6 ratio being smaller for the s case. Analogously, for photon energies (s-polarization) where bands 2 and 3 are nearly degenerate ($h\nu \geq 18$ eV), this feature is seen to be weaker in comparison to bands 5 and 6; such

behavior is least ambiguous for $h\nu \geq 22$ eV. From the spectra at 15 to 17 eV, the band 4 peak is seen to be larger in comparison to that of band 5 for s-polarized light. Finally, there is the seeming absence of the band 3 peak for s-polarization, $h\nu$ = 13 to 15 eV. Taken together, these results lead to the conclusion that bands 3 and 5 are suppressed for s-polarization relative to bands 2, 4, and 6, or the alternate interpretation, that bands 2, 4, and 6 are suppressed for p-polarized light.

To distinguish between these possibilities, we must turn to group theory. The general selection rule for transitions is of course well-known[19]: For initial and final states transforming as Γ_i and Γ_f, and a transition operator as Γ_γ, the direct product $\Gamma_f^* \times \Gamma_\gamma \times \Gamma_i$ must contain the identity representation if a transition is to occur. Equivalently, the transition vanishes unless Γ_f is found in $\Gamma_\gamma \times \Gamma_i$, or Γ_γ in $\Gamma_f \times \Gamma_i$.

The initial-state symmetries will be Λ_4, Λ_5, or Λ_6, by analogy to gold.[10] The transition operator is $\vec{A}\cdot\vec{p}$, which reduces to $\vec{\eta}\cdot\vec{r}$; analogous to the nonrelativistic case, this transforms as a vector and we have

$$\vec{\eta} \parallel [111],\ \vec{\eta}\cdot\vec{r} \sim z,\ \Lambda_1 \qquad \text{"p-polarized"}$$
$$\vec{\eta} \perp [111],\ \vec{\eta}\cdot\vec{r} \sim (x,y),\ \Lambda_3 \qquad \text{"s-polarized"}$$

From the character tables of Elliot[20] and Dresselhaus[21] for the double group,

$$\Lambda_1 \times \Lambda_i = \Lambda_i$$

and

$$\Lambda_3 \times \Lambda_i = \begin{cases} \Lambda_3, & i = 1,2 \\ \Lambda_6, & i = 4,5 \\ \Lambda_{1+2+3}, & i = 3 \\ \Lambda_{4+5+6}, & i = 6 \end{cases}$$

The final state is $\Lambda_1 \times D^{1/2} = \Lambda_6$, since it must be symmetric in the limit of reaching the detector.[18] Then we have the selection rules

$$\text{s-polarized} \quad \Lambda_i = \Lambda_4, \Lambda_5, \Lambda_6$$

$$\text{p-polarized} \quad \Lambda_i = \Lambda_6$$

These selection rules are consistent with our data if we take the spectral intensities as evidence of suppression of bands 2, 4, and 6 for p-polarization, and assign the symmetries

Λ_6 - bands 3,5,7

Λ_{4+5} - bands 2,4,6

The calculation of Anderson[12] for Pt does not provide the symmetries of the Λ bands. If we refer to the calculation of Christensen and Seraphim[10] for Au, which should also apply to Pt, we see that these empirical assignments are inconsistent with those given theoretically. In that calculation, however, band 7 is assigned as Λ_4, which in our notation is unreasonable, since the Λ_4 representation is not symmetric under the elements $\bar{E}$, $2C_3$, σ_v, and $\bar{\sigma}_v$ of the

double group; it thus appears that the double group notation of Ref. 10 is different from that of Dresselhaus. The Au band structure of Sommers and Amar,[15] which specifically uses the notation of Elliot, gives initial state assignments different from those of Christensen and Seraphim, and more consistent with those presented here. As noted previously, however, there are several artifacts in that work, such as overlarge d-band width, inaccurate TDOS, and spurious band-crossings, which limits its usefulness. Accordingly, neither theoretical assignment is found to be consonant with that determined experimentally.

V. Thermal Effects in Au(111)

That ARP spectra can undergo dramatic changes with variation of temperature has been well-established in the case of Cu(110).[22] In general, such changes will result from an enhancement of indirect transitions with increasing temperature; this is due to an increase in the number of populated phonon modes and concomitant increase in the number of channels available for phonon-assisted indirect transitions. Correspondingly, cooling of a sample may be expected to enhance the contribution of direct transitions, and for a material such as gold, which has a comparatively low Debye temperature and hence higher susceptibility to indirect processes, one may expect particularly significant changes.

Figures 7 and 8 show spectra for Au(111) at room temperature (ca. 300°K) and cooled to approximately 150°K. It is apparent that the most dramatic changes occur for low photon energies (Figure 7), where the reduction in temperature leads to a marked enhancement of the spectral features over background. There are two mechanisms that could account for this enhanced contrast: reduction of the inelastic background,[23] or enhancement of direct transitions due to a diminution in phonon-assisted indirect transitions.[24] As we shall now discuss, there are features in our spectra which indicate that both mechanisms may be involved.

The primary indication of a reduction in phonon-assisted processes may be taken from the photon energy dependence of the spectra. As the probability for phonon-induced indirect transitions increases with decreasing phonon wavevector,[24] we may think of such processes in first order (i.e., when they contribute only weakly to the spectrum) as producing a net broadening in the initial-state wavevector, or "thermal broadening." The band width ΔE of a feature will depend not only on this Δk but on the region of the zone in which the transition originates. In particular, it will be for those transitions originating at points where the bands are steep that ΔE will most strongly depend on Δk; this is where the largest change upon cooling is expected. Conversely, smaller changes should be apparent on cooling for regions of the zone where the bands are flat. As seen in Figure 4,

it is thus for low photon energies that we expect cooling to have its greatest effect, while by $h\nu$ = 20 eV, as the initial states approach Γ, the spectra should be less affected. That this is precisely the behavior observed in Figures 7 and 8 indicates that a reduction in thermal broadening may be at least partially responsible for the enhancement observed.

There are several other features in these spectra which may be used in attempting to obtain a more complete explanation. We first note the behavior of the surface state intensity at low photon energies; it is clear that this transition is enhanced at low temperatures. Since this feature is dispersionless for normal emission, our discussion above would indicate it to be relatively insensitive to temperature changes. On the other hand, the processes involved in determining the intensity of surface states are poorly understood, and it is quite possible that a competing mechanism, for example surface-phonon-induced indirect transitions, could be the cause of this change. In fact, results of analogous experiments for Ag(111) show a similar enhancement of the surface state,[25] without any other significant changes in the spectral appearance. As silver has a higher Debye temperature than gold, this would tend to indicate that phonon-assisted indirect transitions, which contribute both to the inelastic tail and k-broadening, are less important in Ag, and correspondingly that the mechanism governing surface state intensity losses is less dependent on the bulk properties

of the material involved. This propensity for indirect transitions in Au vis-a-vis Ag is also observed for the other low-Miller-index faces.[26]

The other major feature that provides insight is the intensity of the s-p plateau. We have calculated the ratio of the s-p to d-band intensities, subtracting the apparent background, for both sets of data. As seen in Table IV, these values are virtually identical for both temperatures. The implications of this are twofold. The first is that the mechanism that produces the s-p plateau cannot be that of phonon-induced indirect scattering since this would necessarily lead to a decrease of the s-p to d-band ratio with cooling. It thus appears most likely that the s-p plateau arises from some process analogous to that producing TDOS features, which would be relatively insensitive to changes in temperature. In fact, our spectra contain features that demonstrate this difference in temperature dependence between ODDOS and TDOS processes. As mentioned earlier, the shoulder at the leading edge of the d-bands may be assigned as a TDOS feature; it is seen to be insensitive to cooling. On the other hand, for a ODDOS feature such as that observed as a component of the peak at 6.2 eV, $h\nu$ = 18, which arises due to the flatness of bands (2,3) near Γ, cooling produces a significant diminution of intensity.

The second implication of the thermal independence of the s-p to d ratio is that thermal broadening cannot be the

whole story in explaining the spectral enhancement at low temperatures. If such were the case, the ratio would of necessity drop at low temperatures, due to the enhancement of the d intensity. On the other hand, any mechanism leading to a reduction in the background would leave the ratio unaltered, since the background is subtracted when obtaining this parameter. This strongly suggests that phonon contributions to the inelastic tail must play a strong, and perhaps dominant, role in determining the spectral contrast.

VI. Final-State Effects

While the analysis of our data has to this point concentrated on initial-state features, there are also features in the spectra which give insight into final-state effects. We have already discussed our use of a free-electron-like state for band mapping, and while such a method is quite adequate away from the center or edges of the zone, it becomes suspect where the conduction bands are expected to undergo significant perturbation. Figure 9 shows the theoretical initial- and final-state band structure for Au(111), along with our modified plane-wave final state. As can be seen, band 7 near Γ becomes quite flat, and in fact a gap may be expected between it and the next band, which will have a significant amount of $\vec{G}$ = [888] character. In this region, the exact nature of the final state becomes much less clear. We have accordingly taken spectra for both Pt and Au with a finer

energy mesh in the photon energy range where this part of band 7 is expected to be accessed. As shown in Figures 10 and 11, dramatic intensity resonances occur as the final state approaches Γ. There are two possible explanations for this, the first being associated with the change in dispersion of band 7 near Γ, due to increased f character, and the second with the presence of the gap.

Of these two explanations, only the former is consistent with these data and the results of studies for other faces. Such resonances have already been reported in Ag(111)[4] and Pd(111).[3] Work in our laboratory has also shown their presence in Ag(110) and Ag(100).[27] In all these cases, the RAPW final-state band is quite flat near Γ. For Au(100), however, and by extension for Pt(100), the final-state band near Γ is not flat but rather peaks near $\vec{k}_i$ = (0,2,0) and drops as it approaches Γ. Our studies on Pt(100)[29] show that, unlike for Pt(111), the intensity resonances are quite weak. Were these resonances associated with the gap, such would not be the case.

To more fully examine this behavior, we have calculated normalized intensities for the Λ(2,3) → Λ(7), Λ(4) → Λ(7), and Λ(5,6) → Λ(7) transitions in Au(111) and Pt(111) as a function of photon energy. These are shown in Figures 12 and 13. In both cases, peak areas were corrected for total photon flux and data accumulation time; in the case of Pt, the analyzer transmission function was also known and used.

Unfortunately, recent indications are that the photon density may undergo changes of unknown magnitude with energy on the 8° line, so that our results could contain an associated error. Such a correction would be expected to be monotonic, however, and hence would alter only the shape and not the existence or location of the resonances. While these results cannot be presumed quantitatively definitive, therefore, they should be qualitatively correct.

As the figures show, all three transitions undergo resonances in intensity with photon energy, with the $\Lambda(5,6) \rightarrow \Lambda(7)$ resonance being the least intense. In the case of Pt, the resonance is consistent for all three transitions, and yields an energy of $E_7(\Gamma) = +16.6$ eV relative to E_F. For gold, the $\Lambda(5,6)$ transition is ca. 1 eV too low, and using the remaining two values yields $E_7(\Gamma) = +16.4$ eV. This latter value compares not unfavorably with the theoretical value of 15.6 eV.[30] It is also interesting to note, especially for Pt, the asymmetry of the resonance, with the line edge being sharper on the gap side. This is a pleasing result; as itinerant final states are rigorously forbidden in the gap in the limit of an infinite solid, one would expect an effect due to bulk bands to disappear more rapidly in the gap. In other words, the width of the final state may be expected to be asymmetric, with a smaller value on the gap side. Unfortunately, a monochromator-derived function could also produce such an asymmetry, and elucidation of this effect

must await more definitive experiments.[31]

The other final-state effect of interest is a constant kinetic energy feature, in both Au and Pt, satisfying the equation $E_B \approx h\nu - 16$. Analogous behavior was observed in Ag(111),[4] and was attributed to scattering and subsequent ejection of electrons of higher kinetic energy into the very high density of states region at 16 eV above E_F, composed of bands 7 and 8. We note that as $h\nu$ decreases, this feature should proceed to lower apparent binding energy, merging with the band (2,3) resonance; this is clearly observed in both crystals. It is interesting that this feature appears stronger here than in Ag; comparison of the RAPW calculations for Ag and Au shows that both bands 7 and 8 are flatter near Γ in Au, which accounts for the intensity difference and lends further credence to the mechanism proposed.

We have also studied the behavior of this feature in Pt(111) for off-normal emission. As seen in Figure 14, the peak is most intense at normal, and falls off symmetrically about the (111) axis, having disappeared by a 15° takeoff angle. This would lead one to suspect that it is the flatness of band 8, which is unique to the Λ direction, and not just that of band 7 near Γ, which provides the high conduction band density-of-states necessary for this process. In fact, in Ag(100)[27] and Pt(100)[29] no such constant kinetic energy feature is observed, although resonances in direct transition intensities, analogous to those reported in Ag(111), are

observed. Taken together, these observations strongly indicate a mechanism that involves scattering into the $\Lambda(8)$ band, followed by crossing to $\Lambda(7)$ and subsequent emission from the crystal.

VII. Summary and Conclusions

We have presented results of normal emission ARP studies for variable photon energy. Specifically, we have mapped bands along most of the Λ line for Pt and Au. Comparison of these results to theory shows that, unlike for simpler cases, the predicted band structures do not agree within experimental error with the empirically derived dispersion relations. Several other aspects of the spectra have been noted and discussed, including a surface state, constant kinetic-energy feature, and density-of-states features. By investigating the effect of cooling for Au(111), we have been able to gain some insight into the mechanisms giving rise to the "s-p plateau" and determining the spectral contrast, as well as distinguishing one- and three-dimensional density-of-states features. Through the use of polarization selection rules and our observed spectral intensities, we have determined the initial state symmetries for Pt(111). We have also investigated resonances in the transition probabilities due to final-state effects.

It is clear that this work, in combination with that cited for Cu, Pd, Ni, and Ag,shows that the use of ARP data,

in conjunction with the direct-transition model and an appropriate final state, provides a method of general utility for mapping bands in (111) single crystals. The logical extension of such studies is to other low-Miller-index crystal faces, and such work is presently underway. Other avenues of investigation that this work opens are the use of polarization effects to assign initial-state symmetries for relativistic band structures, and the elucidation and characterization of final-state resonances. The latter subject, in particular, is of considerable interest, as it should shed light on the exact nature of the final state near--and in--gaps predicted for the infinite solid limit.

ACKNOWLEDGMENTS

We wish to thank Professor G. Somorjai for supplying the Au single crystal used as the starting material in this study. One of us (KAM) wishes to thank D.R. Denley for helpful discussions concerning polarization selection rules.

This work was supported by the Division of Chemical Science, Office of Basic Energy Sciences, U.S. Department of Energy under Contract No. W-7405-Eng-48. It was performed at the Stanford Synchrotron Radiation Laboratory, which is supported by the NSF Grant No. DMR 77-27489, in cooperation with the Stanford Linear Accelerator Center.

References

1) J. Stöhr, P.S. Wehner, R.S. Williams, G. Apai, and D.A. Shirley, Phys. Rev. B17, 587 (1978); J. A. Knapp, F.J. Himpsel, and D.E. Eastman, Phys. Rev. B19, 4952 (1979); P. Thiry, D. Chandesris, J. Lecante, C. Guillot, R. Pinchaux, and Y. Petroff, Phys. Rev. Lett. 43, 82 (1979).

2) D.E. Eastman, F.J. Himpsel, and J.A. Knapp, Phys. Rev. Lett. 40, 1514 (1978); F.J. Himpsel, J.A. Knapp, and D.E. Eastman, Phys. Rev. B19, 2919 (1979).

3) F.J. Himpsel and D.E. Eastman, Phys. Rev. B18, 5236 (1978).

4) P.S. Wehner, R.S. Williams, S.D. Kevan, D. Denley, and D.A. Shirley, Phys. Rev. B19, xxxx, and references therein.

5) G.V. Hansson and S.A. Flodstrom, Phys. Rev. B18, 1572 (1978).

6) P. Heimann, H. Miosga, and H. Neddermeyer, to be published, 1.

7) J. Stöhr, G. Apai, P.S. Wehner, F.R. McFeely, R.S. Williams, and D.A. Shirley, Phys. Rev. B14, 5144 (1976); P.S. Wehner, PhD Thesis, Univ. of Calif., Berkeley, April 1978 (LBL-7622).

8) A more complete description will be published in the near future.

9) P. Heimann, H. Miosga, and H. Neddermeyer, to be published, 2.

10) N.E. Christensen and B.O. Seraphim, Phys. Rev. B4, 3321 (1971).

11) P.H. Citrin, G.K. Wertheim, and Y. Baer, Phys. Rev. Lett. 41, 1425 (1978).

12) O.K. Anderson, Phys. Rev. B2, 883 (1970).

13) S.D. Kevan, K.A. Mills, R.S. Williams, and D.A. Shirley, unpublished data.

14) N.E. Christensen, Phys. Rev. B13, 2698 (1976).

15) C.B. Sommers and H. Amar, Phys. Rev. 188, 1117 (1969).

16) D.A. Shirley, Phys. Rev. B5, 4709 (1972).

17) F. Hermann and S. Skillman, Atomic Structure Calculations (Prentice Hall, Englewood Cliffs, New Jersey 1963).

18) J. Hermanson, J. Anderson, and G. Lapeyre, Phys. Rev. B12, 5410 (1975).

19) M. Tinkham, Group Theory and Quantum Mechanics (McGraw Hill, New York, 1974).

20) R.J. Elliot, Phys. Rev. 96, 280 (1954).

21) G. Dresselhaus, Phys. Rev. 100, 580 (1955).

22) R.S. Williams, P.S. Wehner, J. Stöhr, and D.A. Shirley, Phys. Rev. Lett. 39, 302 (1977).

23) J.M. Ballantyne, Phys. Rev. B6, 1436 (1972); B.L. Henke, J. Liesegang, and S.D. Smith, Phys. Rev. B19, 3004 (1979).

24) N.J. Shevchek, J. Phys. C, L555 (1977) and Phys. Rev. B16, 3428 (1977).

25) D.R. Denley, PhD Thesis, Univ. of Calif., Berkeley, July 1978 (LBL-9482). We note that the possibility of surface reconstruction with cooling cannot be entirely ruled out; it is, however, highly unlikely for the (111) face. In addition, studies have shown the surface state to be most intense for this face (Ref. 9), so that reconstruction would be expected to lead to diminution, not enhancement.

26) G.V. Hansson and S.A. Flodstrom, Phys. Rev. B17, 473 (1978), and Ref. 5.

27) K.A. Mills, R.F. Davis, R. Watson, G. Thornton, and D.A. Shirley, to be published.

28) N.E. Christensen, Phys. Stat. Sol. B 54, 551 (1972), and Ref. 10.

29) G. Thornton, R.F. Davis, K.A. Mills, and D.A. Shirley, to be published.

30) J. Hermanson, J. Anderson, and G. Lapeyre, Phys. Rev. B12, 5410 (1975), have studied this effect using angle-integrated CIS spectroscopy and report 15 eV $\leq E_7(\Gamma) \leq$ 16 eV. Their experiment, however included the $\Lambda(5,6) \rightarrow \Lambda(7)$ transition, which we see here to give a characteristically low value for $E_7(\Gamma)$.

31) A recent investigation of Cu(110) [E. Dietz and F.J. Himpsel, Solid State Comm. 30, 235 (1979)] has shown the presence of similar final-state resonances in this material. They have interpreted their results in terms

of a cessation of dispersion for band gap photoemission; our work on Ag(110) (Ref. 27) does not agree with this interpretation, and discusses the question of gap photoemission in detail. For the study conducted here, the flatness of the valence bands near Γ, where the only gap is expected, renders this question unimportant.

32) N.E. Christensen, Phys. Rev. B14, 3446 (1976).

33) N.E. Christensen, Phys. Stat. Sol. B 54, 551 (1972).

34) G.A. Burdick, Phys. Rev. 129, 138 (1963).

35) C.S. Wang and J. Calloway, Phys. Rev. B15, 298 (1977).

Table I

Values of Valence Bands Along Λ in Platinum and Gold (eV)

k (units of Ref. 10)		Energy (eV)					
		Band 1	Band 2	Band 3	Band 4	Band 5	Band 6
000 (Γ)	Au	-	5.90	5.90	4.45	3.55	3.55
	Pt	-	4.07	4.07	2.80	1.40	1.40
111	Au	-	5.90	5.90	4.45	3.95	3.48
	Pt	-	4.15	3.98	2.78	1.75	1.16
222	Au	-	6.15	5.65	4.55	3.60	2.90
	Pt	-	4.05	3.65	3.00	1.10	0.55
333	Au	6.85	6.30	4.95	3.90	2.85	2.50
	Pt	5.65	-	-	2.05	0.40	-
Λ_{min}[a]	Au	7.10 (2.40)	6.45 (2.75)	5.90 (0.00)	4.65 (2.50)	3.95 (1.15)	3.55 (0.00)
	Pt	6.10 (2.30)	4.07 (0.00)	4.07 (0.00)	3.05 (2.10)	- (0.95)	1.40 (0.00)

[a]Value in parenthesis is k_x corresponding to the binding energy at which the band is most tightly bound.

Table II

Derived Crystal Field Parameters

Source	Parameter	Crystal	
		Au	Pt
Experimental fit (eV)	ξ_{5d}	.71 ± .05	.66 ± .05
	10Dq	1.22 ± .05	1.78 ± .05
Force fit (eV)[a]	ξ_{5d}	.74	.63
	10Dq	1.28	1.70
Theoretical fit (eV)[b]	ξ_{5d}	.56	.59
	10Dq	1.36	1.93

[a]Using the value of ξ_{5d} from atomic structure calculations (Ref. 14).

[b]Using splittings at Γ from RAPW calculations (Refs. 10,12).

Table III

Values of 10Dq for Various Transition Metals

		Ni	Cu	Pd	Ag	Pt	Au
10Dq	Expt.	0.7[b]	0.73	1.40[c]	.865	1.78	1.22
	Thy.	1.13	0.8	1.44	.880	1.93	1.36
Ref.	Expt.	2	1	3	4	a	a
	Thy.	35	34	32	28	12	10

[a]This work.

[b]This value may be anomalous as discussed in the text.

[c]Value ignoring spin-orbit splitting (i.e., $\Gamma_{12} - \Gamma_{25'}$).

Table IV

Ratio of s-p Intensity to d-Band Intensity at 300° and 150°K

Photon energy	Intensity ratio[a]	
	300°	150°
9	.37	.46
12	.11	.12
15	.08	.07
18	.05	.06
21	.03	.04

[a]Estimated uncertainty is 20%.

Figure Captions

Figure 1. Experimental geometries employed: (a) "p-polarized" radiation. For gold, a = $[\bar{1}\bar{1}2]$, b = $[\bar{1}10]$, $\theta_p = 62.7°$. For Pt, a = $[\bar{1}10]$, b = $[11\bar{2}]$, $\theta_p = 60°$. (b) "s-polarized" radiation.

Figure 2. Selected photoemission spectra at normal emission for Au(111) in the energy range $6 \leqslant h\nu \leqslant 33$ eV.

Figure 3. Selected spectra, normal emission and p-polarized radiation, for Pt(111) in the energy range $8 \leqslant h\nu \leqslant 33$ eV.

Figure 4. Empirical (circles) and theoretical (solid lines, Ref. 10) valence-band dispersion relations in Au(111). A partial photon energy scale is indicated along the top.

Figure 5. Empirical (circles) and theoretical (Ref. 12) valence bands for Pt(111).

Figure 6. Comparison of spectra for Pt(111) using s- and p-polarized light, for selected photon energies.

Figure 7. Spectra at 300°K and 150°K of Au(111), in the low photon energy region.

Figure 8. Au(111) spectra for higher photon energies at 300°K and 150°K.

Figure 9. Theoretical band structure (solid lines, Ref.10) and the fitted quasi-plane-wave final state used here (solid circles) for Au along the Λ line. Bands are numbered sequentially starting at the lowest energy.

Figure 10. Selected spectra with a finer photon energy mesh for Au(111). Note particularly the resonances in intensity of the main features as $h\nu$ changes.

Figure 11. Spectra of Pt(111) using a smaller energy step. The band (2,3) and (4) resonances may be followed in this figure.

Figure 12. Plot of intensities of the band (2,3) (4), and (5,6) peaks for Pt(111) as a function of photon energy. Approximate maxima are indicated; the ordinate is the relative intensity for a given peak, normalized to its maximal value.

Figure 13. Normalized intensities for the (2,3), (4), and (5,6) peaks in Au(111) as a function of photon energy.

Figure 14. Spectra of Pt(111), p-polarized radiation at 26 eV, for various electron takeoff angles relative to the surface normal. In the geometry of Figure 1a, the angle θ_e corresponds to

takeoff directions in the plane defined by the [111] and [11$\bar{2}$] directions, with Θ_e being negative for rotations towards [11$\bar{2}$]; ϕ_e corresponds to directions in the [$\bar{1}$10] - [111] plane, being negative for rotations towards [$\bar{1}$10]. (a) polar dependence, $\phi_e = 0$. Θ_p is fixed at 60°. (b) azimuthal dependence, $\Theta_e = 0$. Θ_p is fixed at 60°. The dashed line is for E_k = 16 eV.

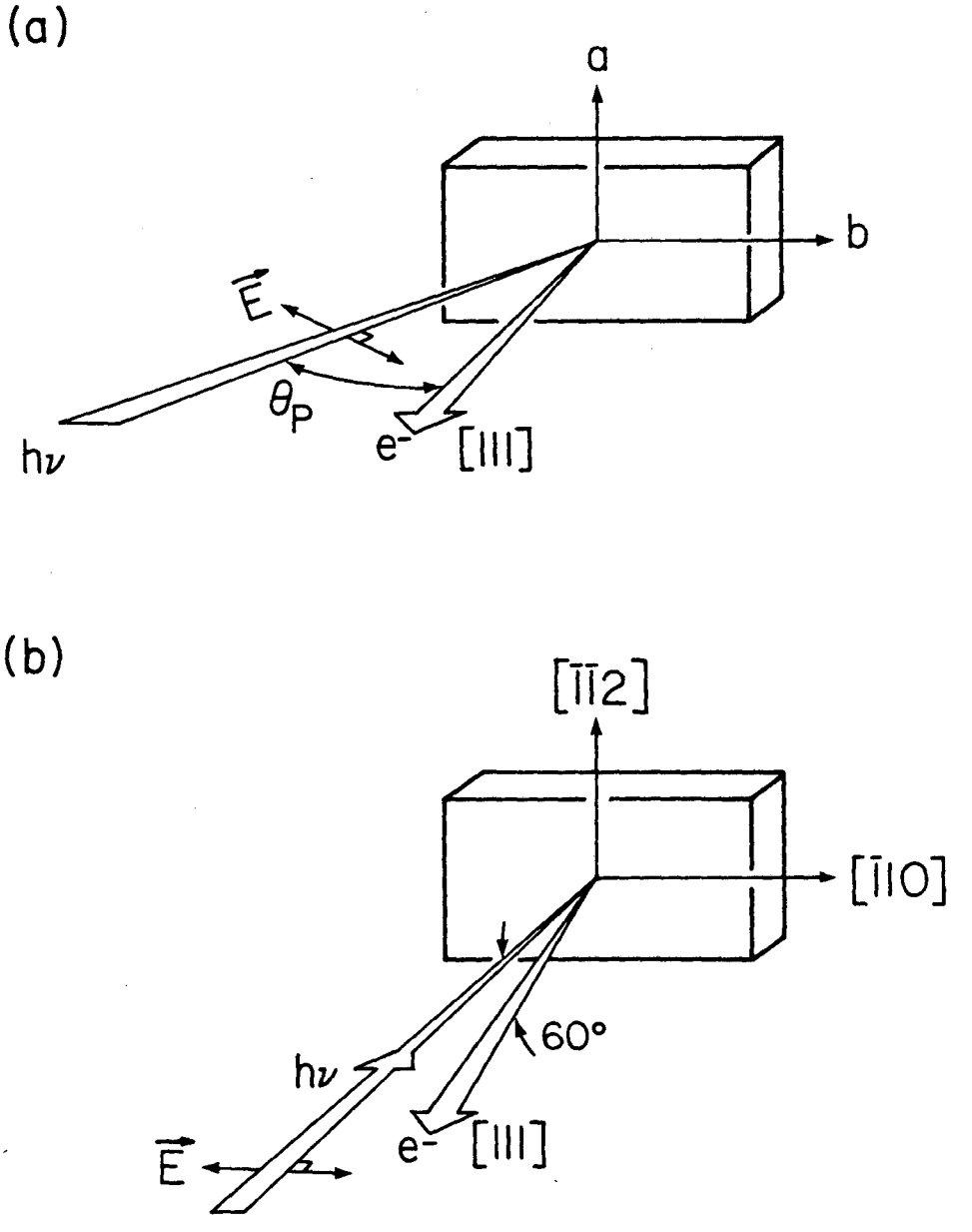

XBL 797-2119

Figure 1

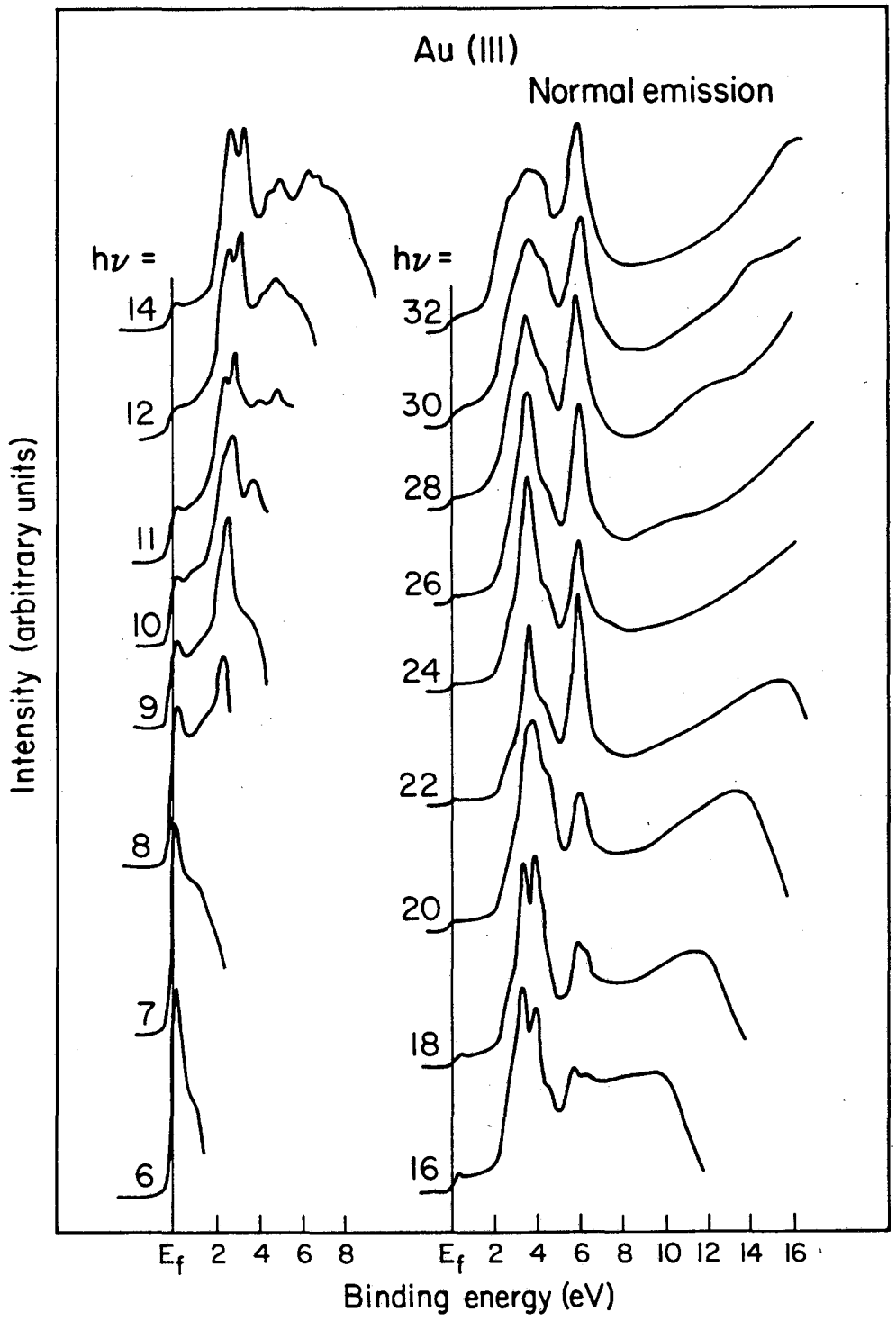

XBL 797-2111

Figure 2

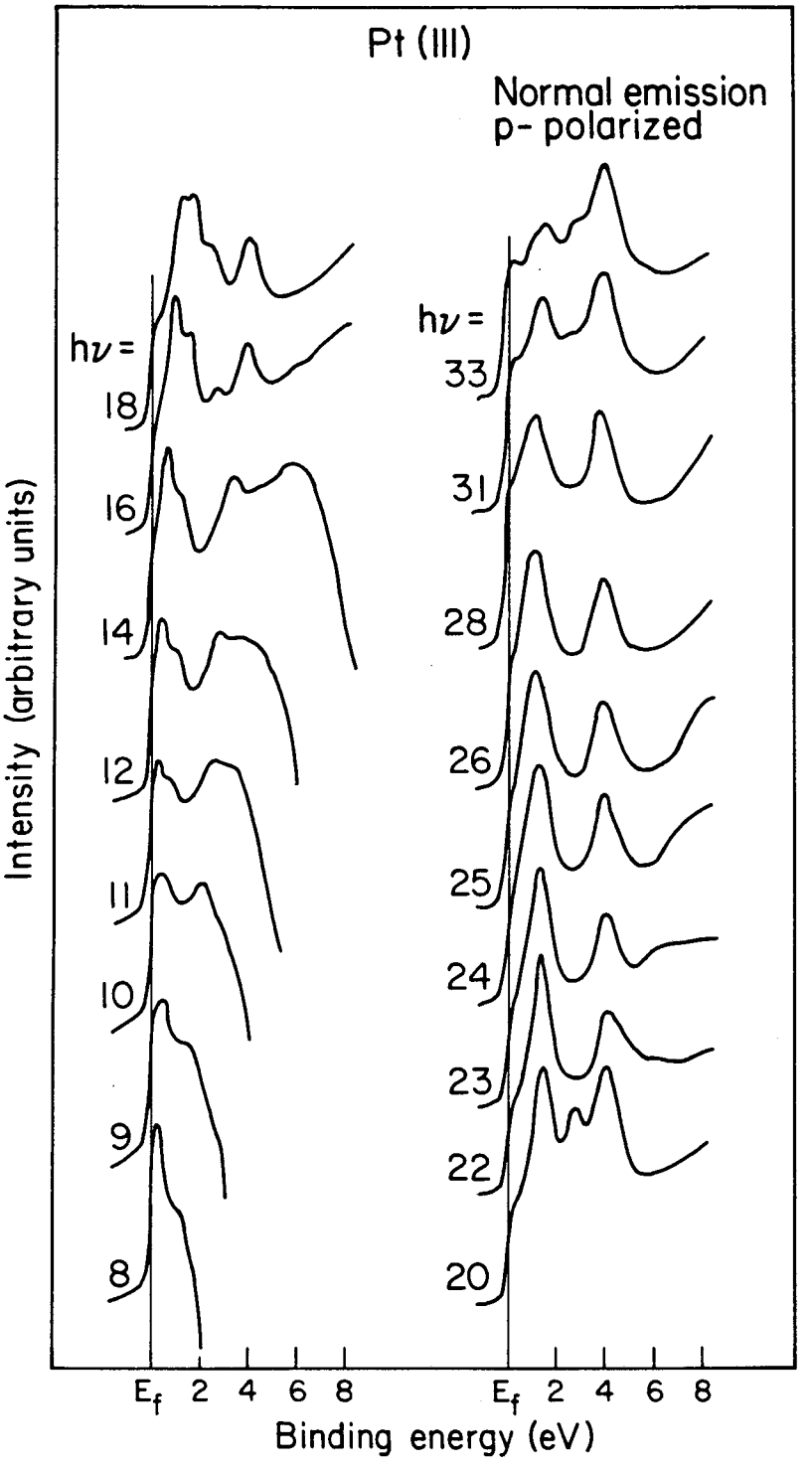

XBL 797-2112

Figure 3

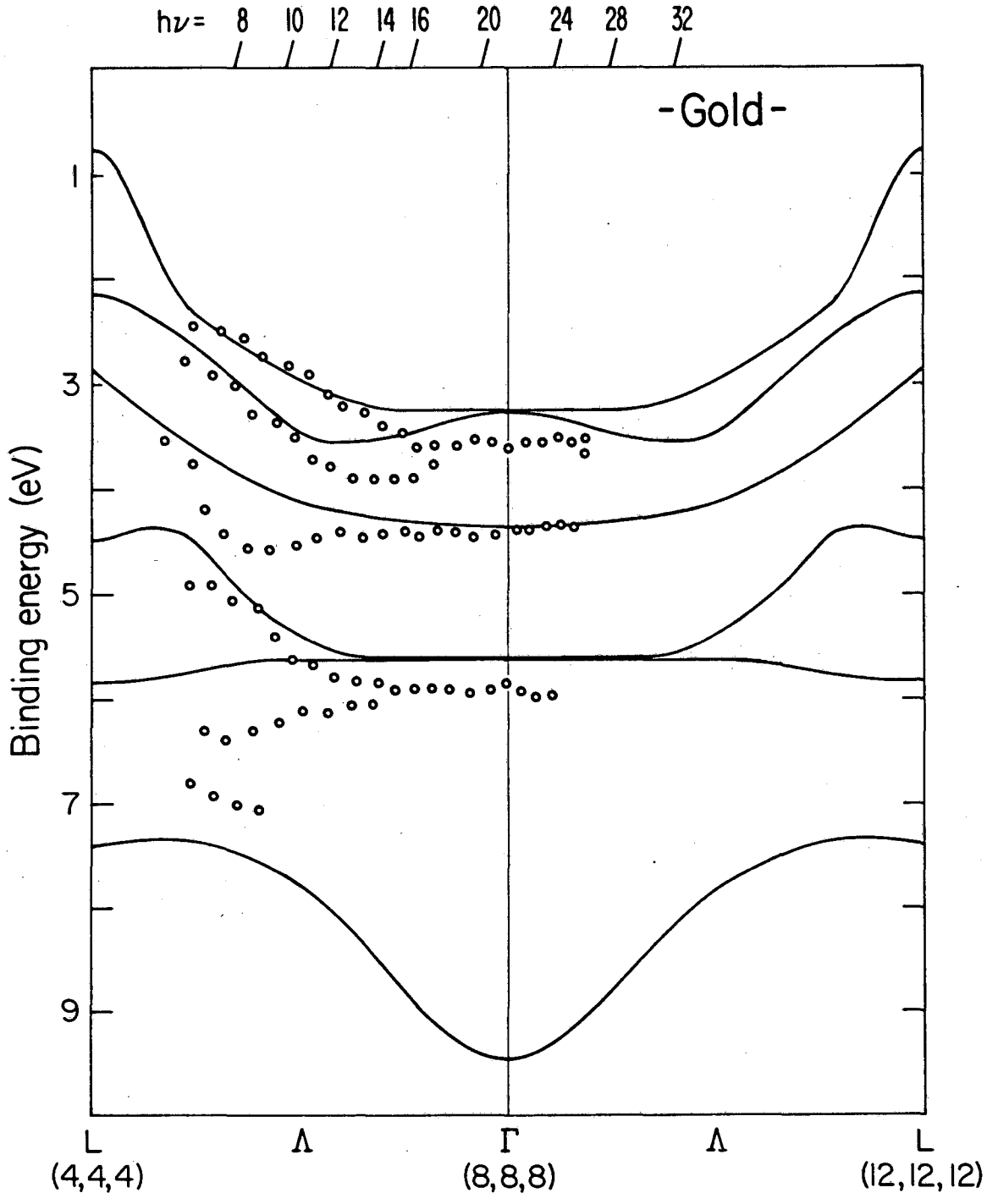

XBL 797-2117

Figure 4

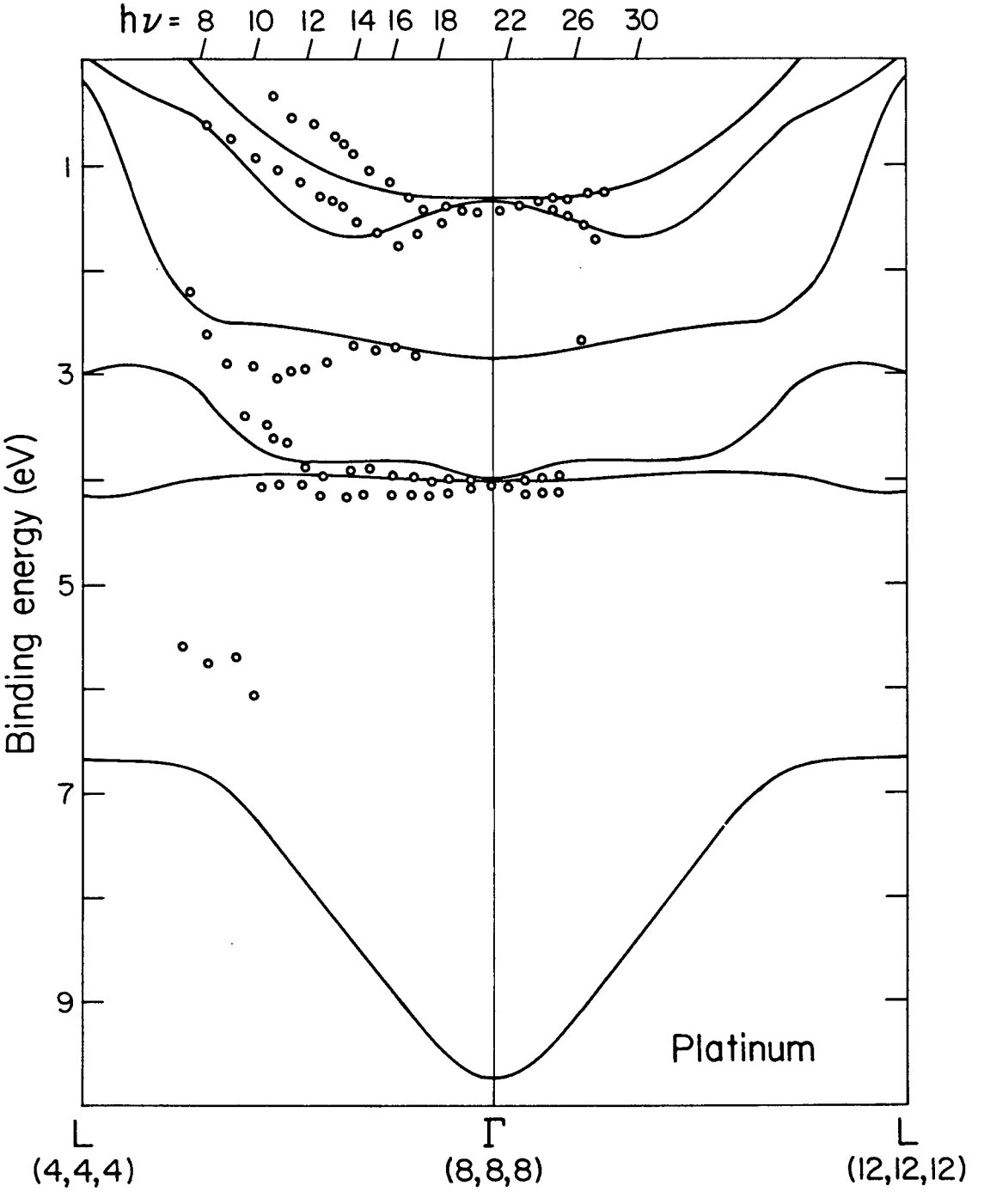

XBL 797-2109

Figure 5

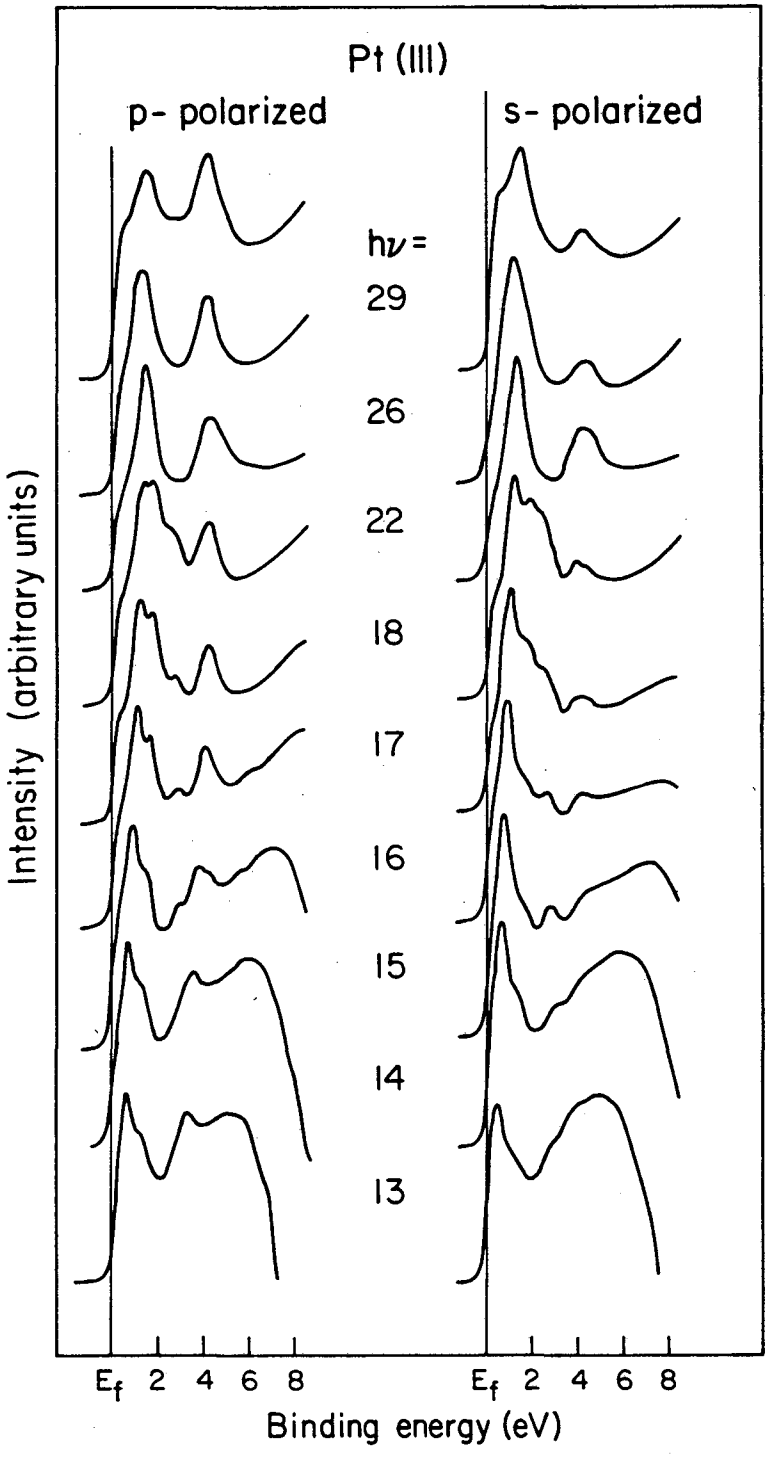

XBL 797-2108

Figure 6

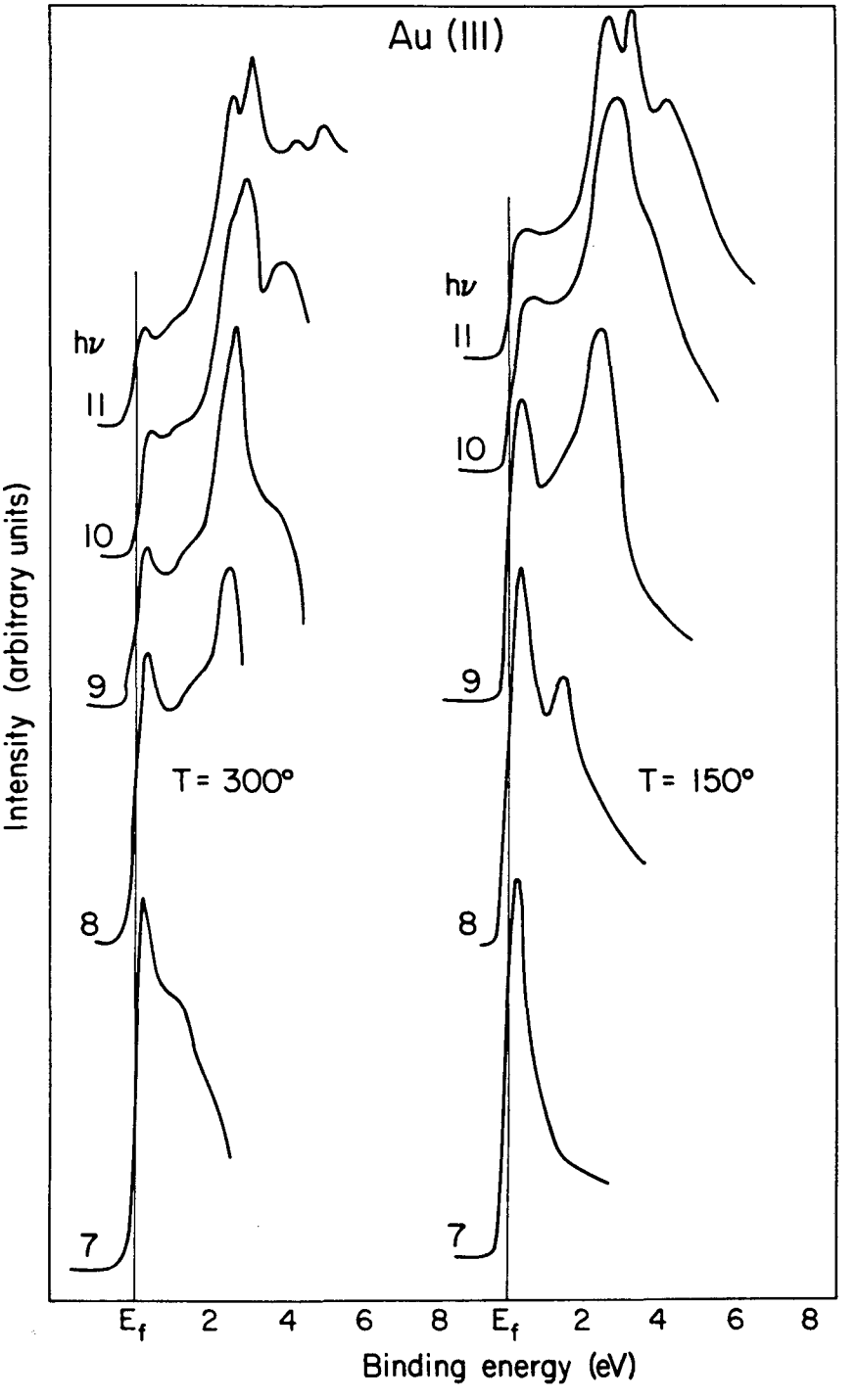

XBL 797-2107

Figure 7

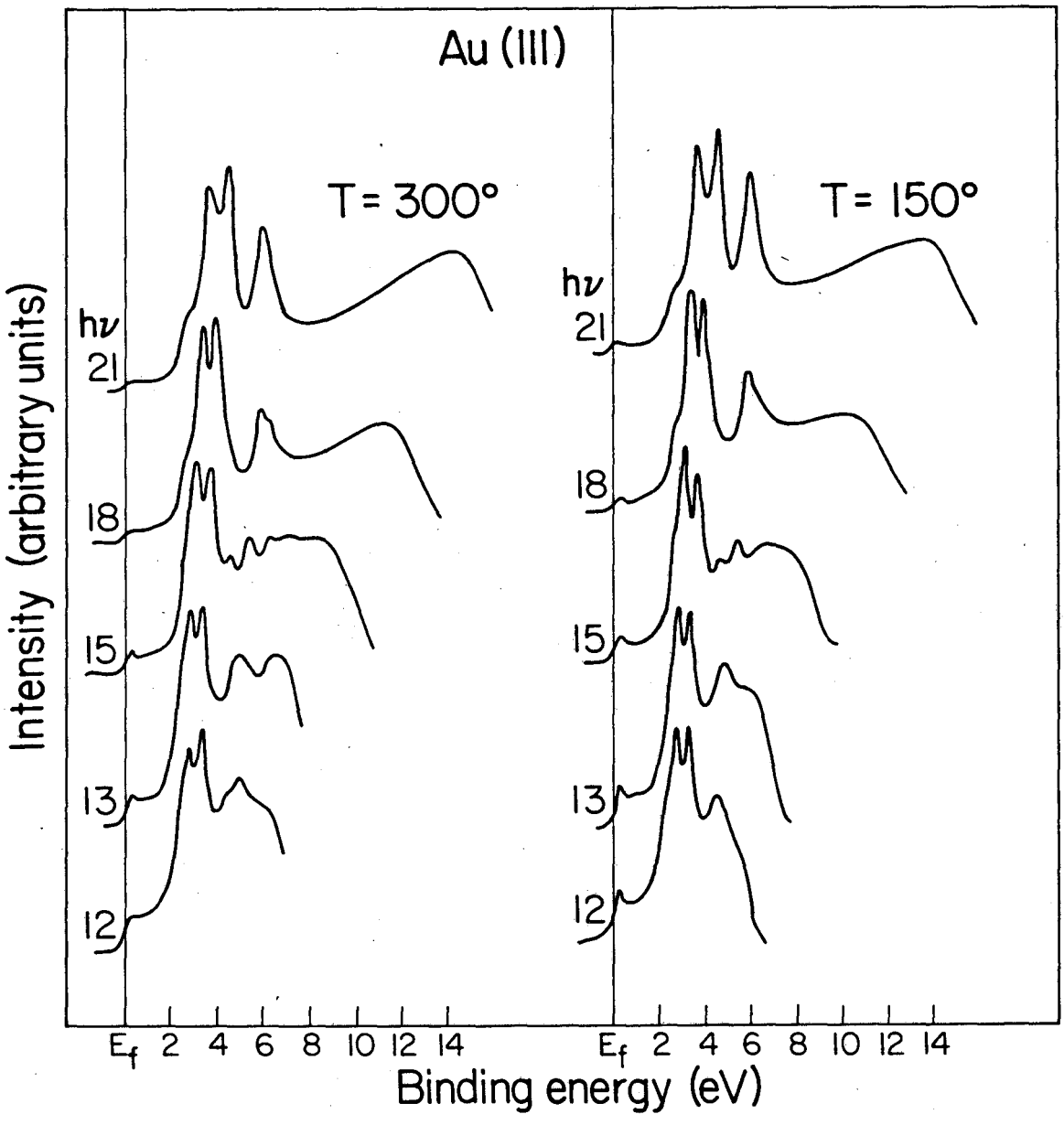

XBL 797-2113

Figure 8

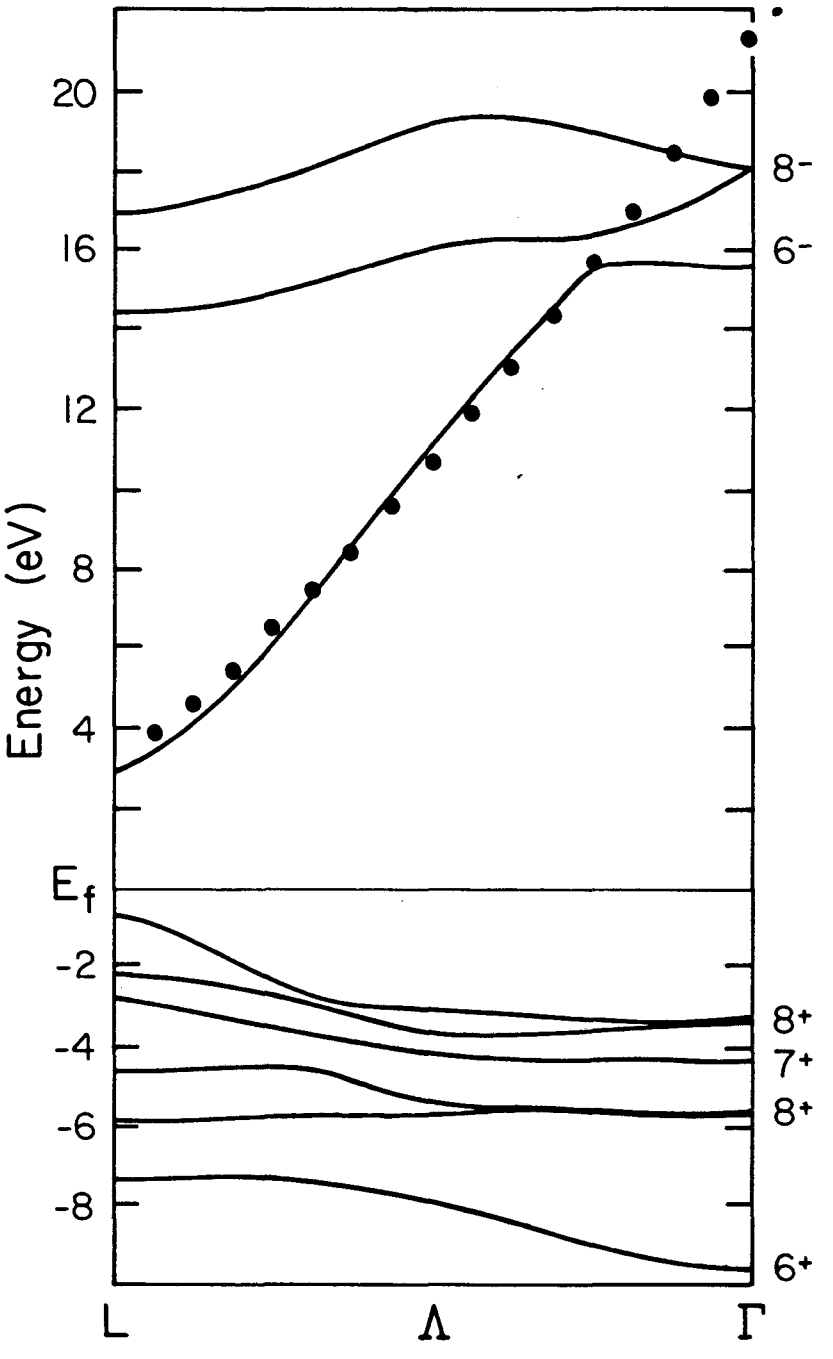

XBL 797-2110

Figure 9

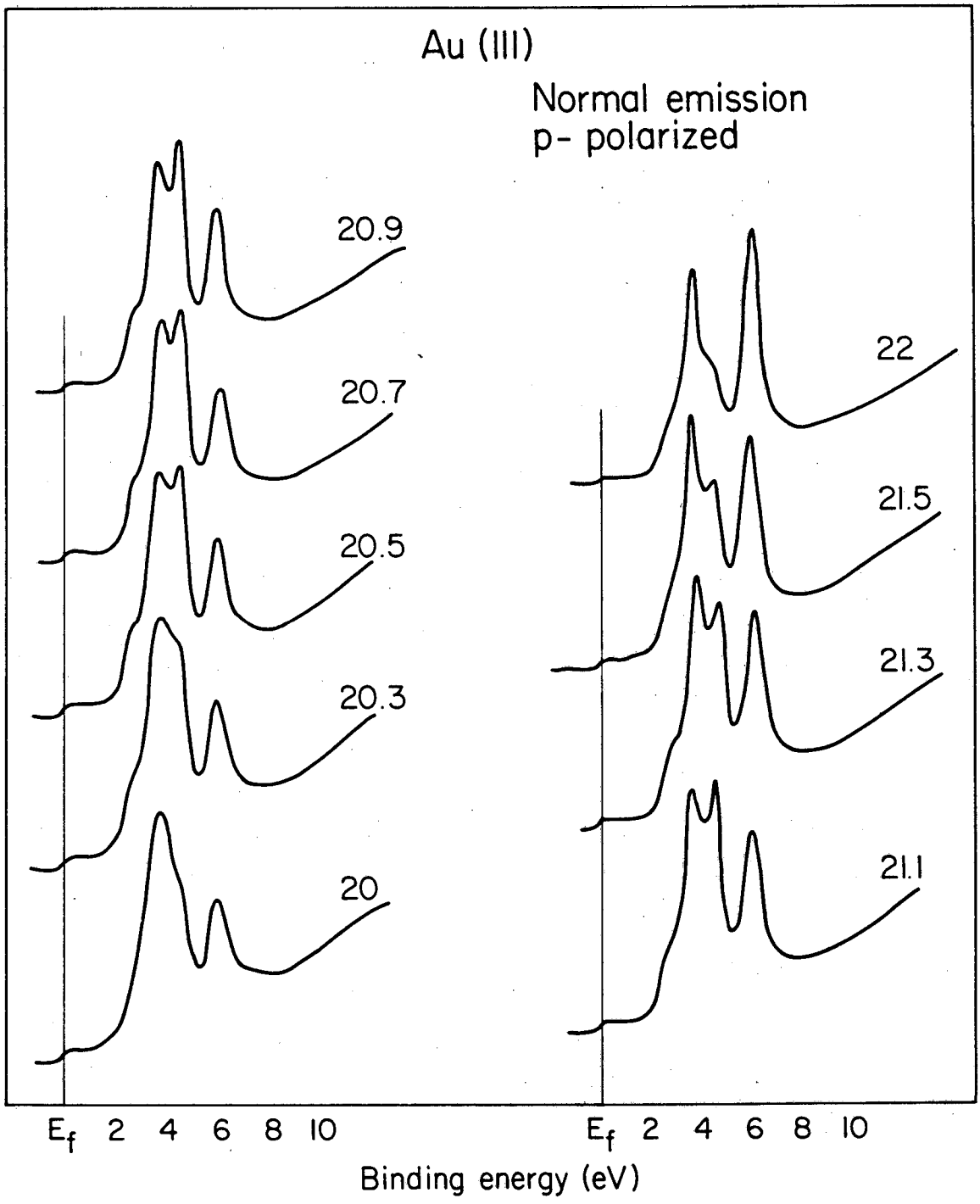

XBL 797- 2115

Figure 10

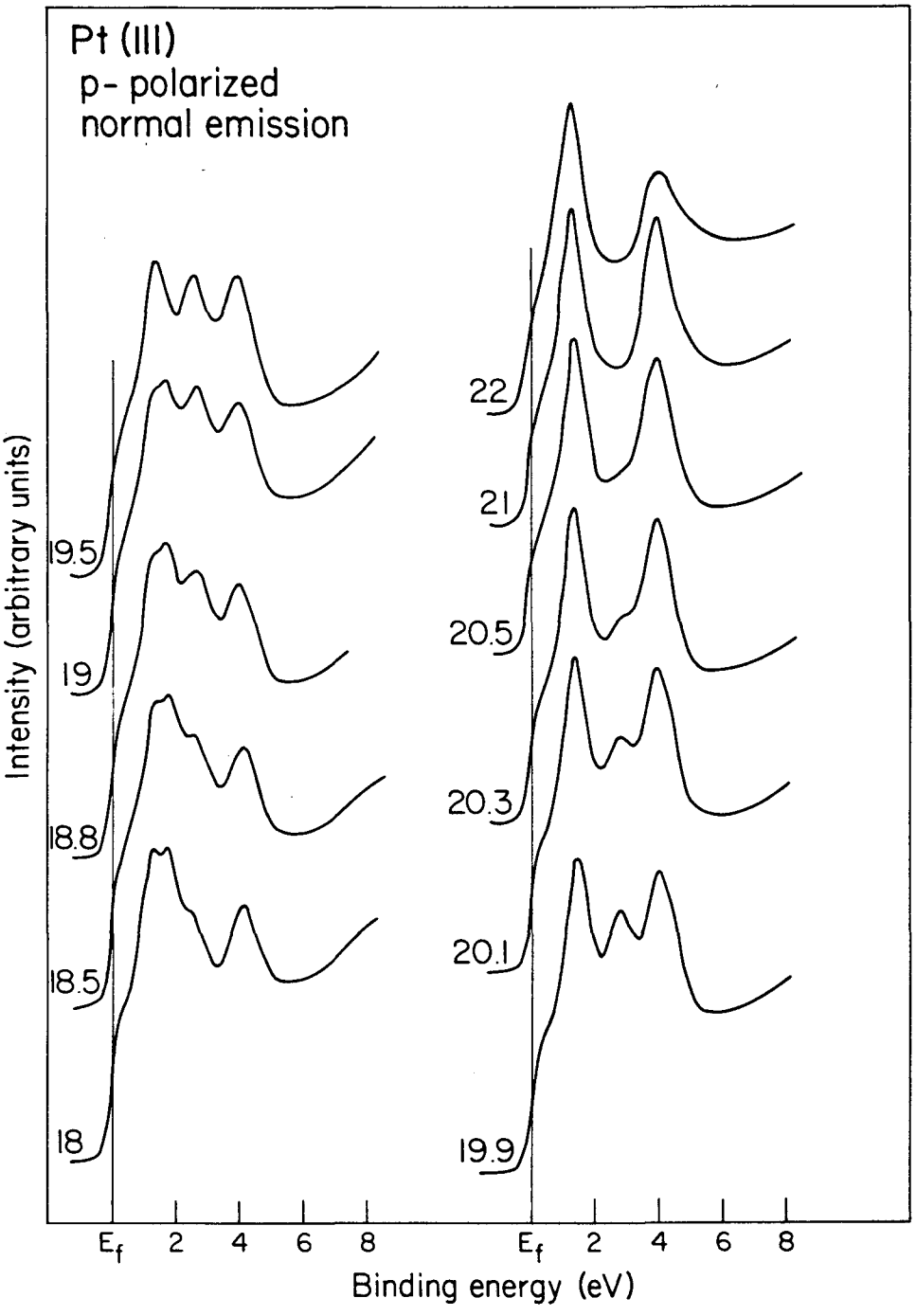
Pt (III)
p- polarized
normal emission
Intensity (arbitrary units)
19.5
19
18.8
18.5
18
22
21
20.5
20.3
20.1
19.9
E_f
2
4
6
8
E_f
2
4
6
8
Binding energy (eV)
XBL 797-2116

Figure 11

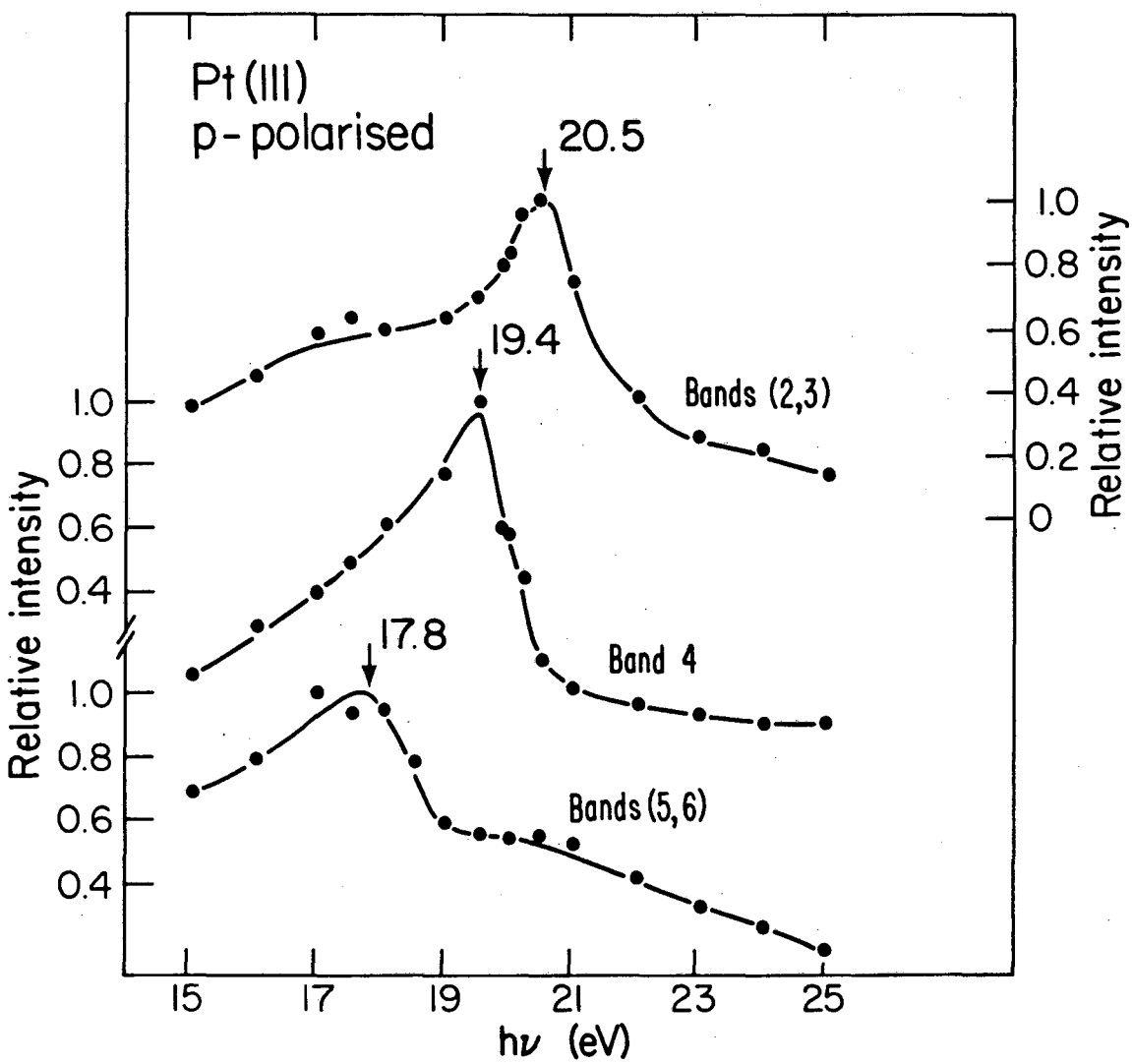

XBL 797-2105

Figure 12

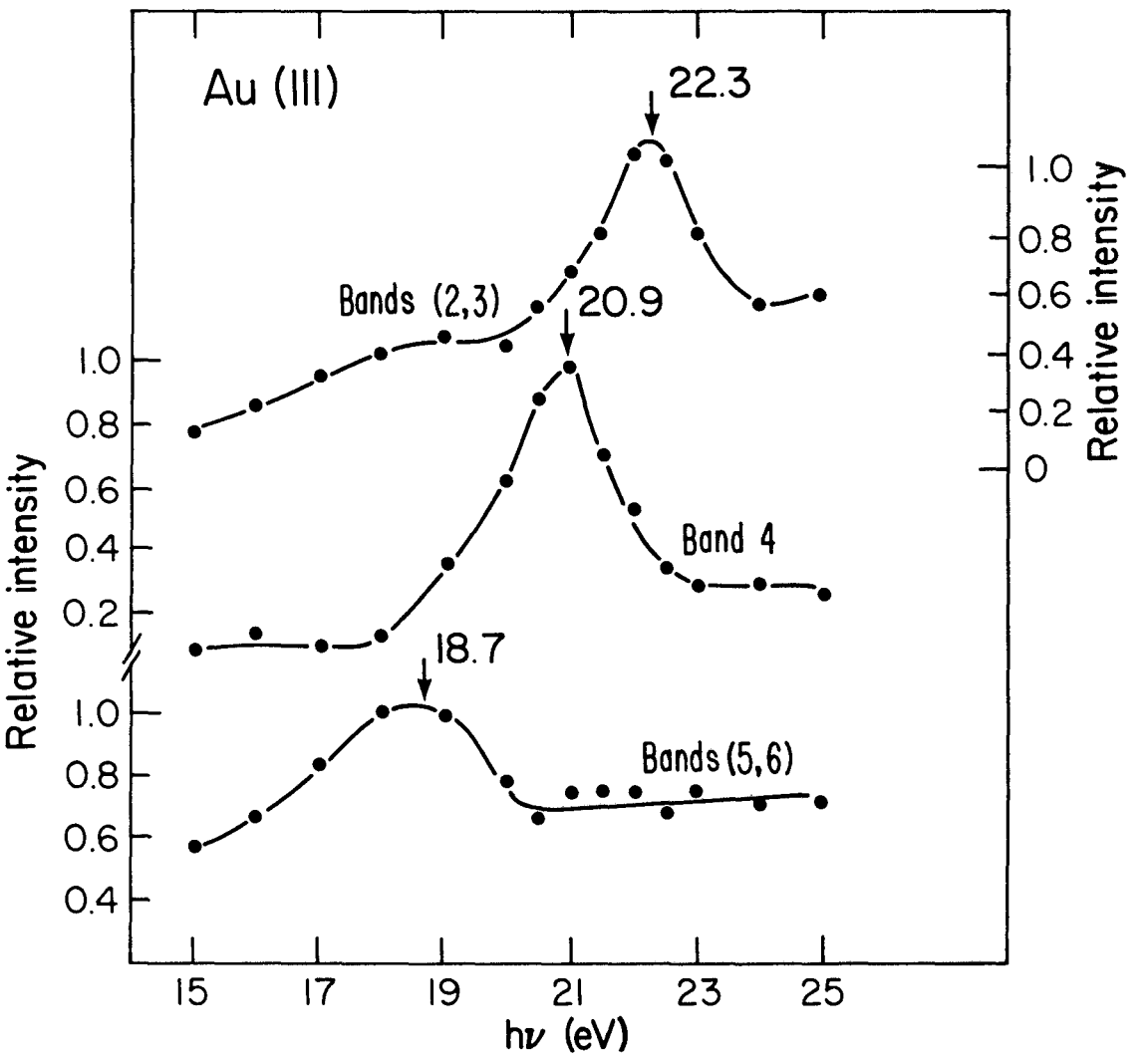

XBL 797-2106

Figure 13

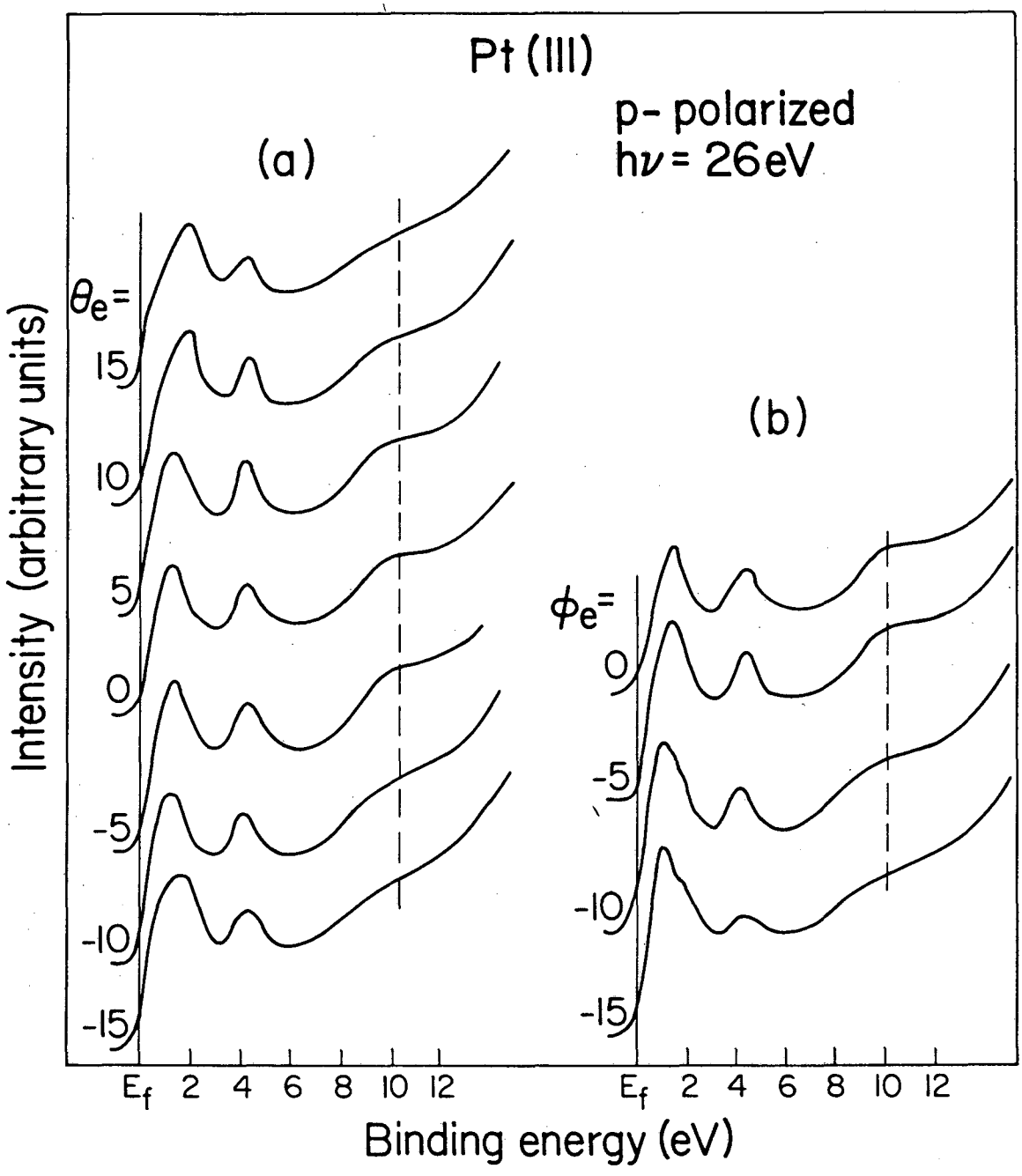

XBL 797-2114

Figure 14

TECHNICAL INFORMATION DEPARTMENT
LAWRENCE BERKELEY LABORATORY
UNIVERSITY OF CALIFORNIA
BERKELEY, CALIFORNIA 94720